Effect of Single Slat and Double Slat on Aerodynamic Performance of NACA 4415

James Julian[1], Waridho Iskandar[2], Fitri Wahyuni[3], Armansyah[4], Ferdyanto[5]
(Received: 7 May 2022 / Revised: 28 May 2022 / Accepted: 4 June 2022)

***Abstract*— this study uses a Computational Fluid Dynamics (CFD) approach. The main object in this study is NACA 4415 with slat variations. The airfoil used as the slat is Eppler 421. Reynolds number in this study is 3×10^6. This study uses an unstructured mesh with a triangular cell shape with 137824 elements. The use of slats can improve the aerodynamic performance of NACA 4415. NACA 4415 without slat stalled at AoA=16º. Stall on airfoils with a single slat and double slat occurred at AoA=20º. Slat can increase C_l in NACA 4415; however, the difference in C_l increase is not much different when using a single slat or double slat. An airfoil with a single slat, on average, can increase C_l by 20.9129%. The average increase in C_l for an airfoil with a double slat is 25.6878%. Single slat and double slat increase C_d. A single slat increased C_d with an average increase of 26.1109%, and the average increase in C_d for airfoils with double slat was 54.6152%. Single slat can produce a better C_l to C_d ratio than double slat, but the optimum AoA of double slat is 1º higher than single slat. Visualization of fluid flow at AoA=16° shows the fluid flow separation in the airfoil without a slat. The fluid flow separation can be handled well when NACA 4415 is given a single slat or double slat.**

Keywords— airfoil, C_d, CFD, C_l, double slat, NACA 4415, single slat.

I. INTRODUCTION

The aerodynamic capability is highly dependent on the airfoil's shape. There are various airfoil forms available that have been used for various purposes. However, the airfoil still has limitations in its aerodynamic performance. One way to improve the aerodynamic performance of the airfoil is to provide a slat near the airfoil. Slat is one of the most commonly used passive flow controls, especially in aviation. The use of slats on airfoils can provide extra lift force on an airfoil. In addition, the slat can also be used as a passive flow control device. The slat can control the fluid flow by directing the fluid flow to flow toward the main airfoil. In addition to directing the fluid flow, slats can also increase the fluid flow velocity. One of the impacts produced by the slat is that it can reduce or even eliminate fluid flow recirculation that occurs on the upper side of the airfoil [1]. The fluid flow separation causes the fluid flow recirculation [2]. The presence of fluid flow separation is detrimental because it can cause a stall on the airfoil [3].

There is research that discusses airfoils and wings. The research was carried out experimentally and computationally. Experimental research was conducted on towing tanks. Meanwhile, computational research was carried out using Fluent software. The results obtained from this study are that the use of slats is proven to increase C_{lmax} from 1.45 to 2.78. The stall can be delayed from AoA=16° to AoA=24° [4]. A study was conducted to optimize the use of slats. The type of airfoil used as the main airfoil is the NACA 0012 airfoil, with the Reynolds numbers used in these computational studies being 6×10^5 and 7.9×10^6. The conclusion obtained from this research is that slat optimization at Reynolds numbers 6×10^5 and 7.9×10^6 can delay stall and slightly reduce C_d, especially at AoA, which is quite extreme [5].

The research in this paper discusses the effect of using single slat and double slat on the NACA 4415 airfoil. The research was conducted using a Computational Fluid Dynamics (CFD) approach. The Reynolds number used in this study is 3×10^6. In general, NACA 4415 has certain limitations, such as too fast stall conditions, unsatisfactory C_l, and the appearance of flow separation at AoA, which is not too large. Therefore, research is needed to improve the aerodynamic capabilities of NACA 4415. This study aimed to investigate the effect of single slat and double slat on the aerodynamic capabilities of NACA 4415. The effect could be a change in the coefficient of aerodynamic forces. In particular, this research reveals fluid flow characteristics in single slats and double slats.

II. METHOD

A. Flowchart

This research begins by conducting a literature study; through a literature study, it can be found several things that can be used as reference sources, aerodynamic data, and other related data. After conducting a literature study, it can proceed to the next stage. The next stage is to prepare the simulation process by creating geometry and doing the meshing process[6]. The geometry that has

James Julian is with Department of Mechanical Engineering, Universitas Pembangunan Nasional Veteran Jakarta, Jakarta, 12450, Indonesia. E-mail: zames@upnvj.ac.id
Waridho Iskandar is with Department of Mechanical Engineering, Universitas Pembangunan Nasional Veteran Jakarta, Jakarta, 12450, Indonesia. E-mail: waridho.iskandar@upnvj.ac.id
Fitri Wahyuni is with Department of Mechanical Engineering, Universitas Pembangunan Nasional Veteran Jakarta, Jakarta, 12450, Indonesia. E-mail: fitriwahyuni@upnvj.ac.id
Armansyah is with Department of Mechanical Engineering, Universitas Pembangunan Nasional Veteran Jakarta, Jakarta, 12450, Indonesia. E-mail: armansyah@upnvj.ac.id
Ferdyanto is with Department of Electrical Engineering, Universitas Pembangunan Nasional Veteran Jakarta, Jakarta, 12450, Indonesia. E-mail: ferdy@upnvj.ac.id

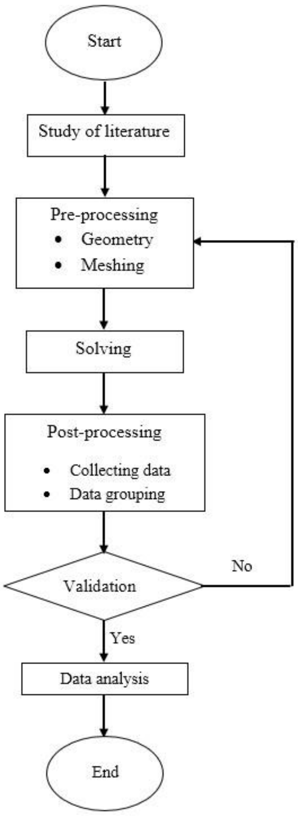

Figure. 1. Research flow chart.

been meshed is then used for the solving stage. The solving stages are carried out using software or better known as CFD. After getting a solution from the meshing process, the process will proceed to the Post-processing stage. The post-processing stage consists of collecting and grouping data. These data are then validated to ensure that the data obtained are valid [7]. If the data is valid, it can proceed to the data analysis process, but if it is not valid, it will return to the Pre-processing stage. Overall the flowchart in this study can be seen in Figure 1.

B. Models Detail

The geometry used in the computational process consists of three models. The first model is the NACA 4415 without a slat; the second model is the NACA 4415 airfoil with a single slat; the last model is the NACA 4415 with a double slat. The airfoil's chord length (c) used for this research is 1 meter [8]. The slat used is an Eppler 421 airfoil with a chord length of 0.16 meters. The slat deflection angle used is -20°. The slat used is an Eppler 421 airfoil with a chord length of 0.16 meters. The slat deflection angle used is -20°. The slat is airfoil. The distance between the first slat's leading edge installed near the leading edge 0.165c from the main and the second slat's leading edge is 0.1c meters. These geometric models are then in the fluid domain with a combined form of semi-circle and rectangle. Size In detail, the geometric models can be seen in Figure 2.

C. Mesh

The type of mesh for computational processes is an unstructured mesh. The shape of the element used is a triangle. The number of elements that make up the mesh is 137824 elements. The mesh around the airfoil is made tightly around the surface of the airfoil [9]. Overall, the mesh details can be seen in Figure 3.

D. Coefficient of lift and drag force

One of the analyzes used in this paper is the analysis of aerodynamic forces. The aerodynamic forces consist of lift and drag forces. The lift force is a force that acts in a direction perpendicular to the direction of the upstream velocity. Meanwhile, the drag force is an aerodynamic force whose direction is parallel to the direction of the upstream velocity [10][11][12]. The aerodynamic forces are given in the form of a dimensionless coefficient [13]. Specifically, the lift coefficient mathematical equation can be seen in equation 1[14], while the drag coefficient is in equation 2 [15].

$$C_d = \frac{d}{\frac{1}{2}\rho U^2 c} \tag{1}$$

$$C_l = \frac{l}{\frac{1}{2}\rho U^2 c} \tag{2}$$

Where, d : drag force, l : lift force, c : chord length, U : Free stream velocity, ρ : Density of fluid

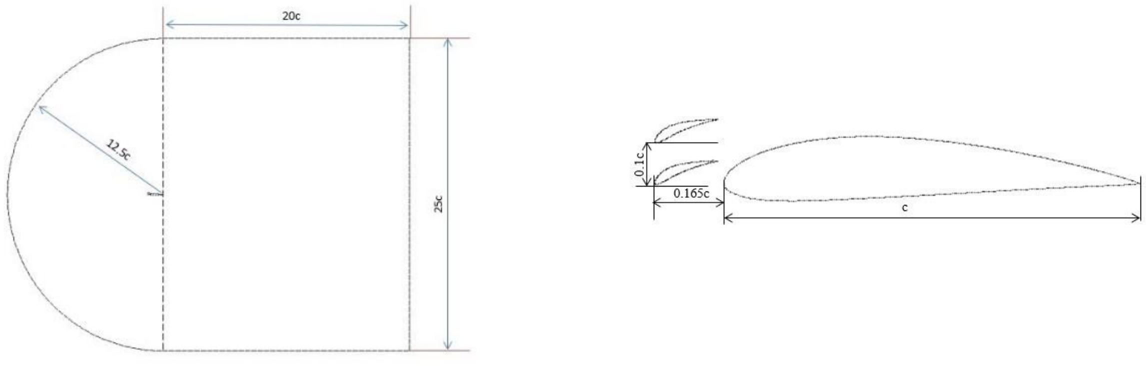

(a) fluid domain (b) Airfoil with slat

Figure. 2. Domain geometries

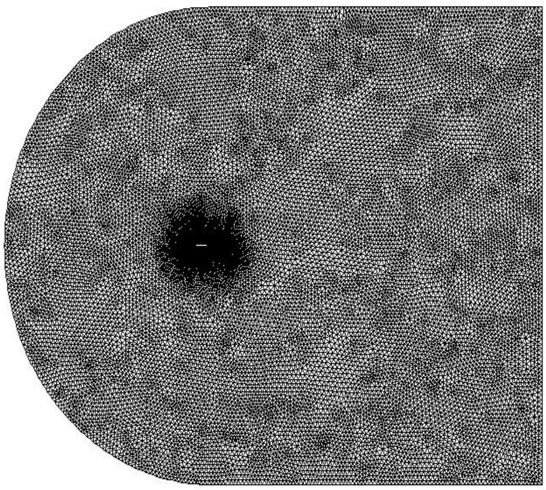

Figure. 3. Mesh used in the computational process

E. Governing equation

The governing equation in this paper is the Reynolds Averaged Navier-Stokes (RANS) equation. The RANS equation is a Navier-Stokes equation that has been modified to be used in CFD applications. The RANS equation is written mathematically in equations 3 and 4[16]. The turbulence model used is $k-\varepsilon$. $k-\varepsilon$ is a turbulence model that is commonly used in computing processes. The mathematical equation of the $k-\varepsilon$ model is in equations 5 and 6[17]. The $k-\varepsilon$ equation is applied in this study because this model has a relatively lower cost per iteration compared to the turbulence models of the other two equations models.

$$\frac{\partial \rho}{\partial t}+\frac{\partial}{\partial x_i}(\rho u_i)=0 \tag{3}$$

$$\frac{\partial}{\partial t}(\rho u_i)+\frac{\partial}{\partial x_i}(\rho u_i u_j)=-\frac{\partial p}{\partial x_i}+\frac{\partial}{\partial x_j}\left[\mu\left(\frac{\partial u_j}{\partial x_i}+\frac{\partial u_i}{\partial x_j}-\frac{2}{3}\delta_{ij}\frac{\partial u_j}{\partial x_j}\right)\right]+\frac{\partial}{\partial x_j}\left(\rho\overline{u_i^{'}u_j^{'}}\right) \tag{4}$$

$$\frac{D}{Dt}(\rho k)=\frac{\partial}{\partial x_j}\left[\left(\mu+\frac{\mu_t}{\sigma_k}\right)\frac{\partial k}{\partial x_j}\right]+G_k-\rho\varepsilon \tag{5}$$

$$\frac{D}{Dt}(\rho \varepsilon)=\frac{\partial}{\partial x_j}\left[\left(\mu+\frac{\mu_t}{\sigma_\varepsilon}\right)\frac{\partial \varepsilon}{\partial x_j}\right]+C_{e1}\frac{\varepsilon}{k}G_k-\rho C_{\varepsilon 2}\frac{\varepsilon^2}{k} \tag{6}$$

III. Results And Discussion

A. Validation

The validation in this paper is carried out by comparing the data obtained from computational results with experimental data obtained from research conducted by Jacobs and Sherman[18]. The comparison data used are C_l and C_d data from NACA 4415 without slat, as shown in Figure 4. Validation of C_l data shows that the computational and experimental results are not too different. At AoA≤13°, the data obtained from the computational results can show very satisfactory results. The computational data showed that the stall condition was 1° faster than the experimental data. A stall on computational data is seen at AoA=16°, while experimental data shows a stall at AoA=17°. After the stall conditions, the data obtained are very different. The difference is caused by the unpredictable airfoil data after the stall condition. The following data validated is the C_d data which represents the drag received by the airfoil. In Figure 4(b), it can be seen that the C_d generated through the computational and experimental processes shows a similar trend where C_d increases with increasing AoA. Overall, both C_l and C_d from the computational results give satisfactory results. Thus, it is concluded that the computational data can be said to be valid data.

B. Analysis

The slat provides additional lift to the airfoil and can be a passive flow control device. In Figure 5, it can be seen that both single slat and double slat can provide an extra lift on the airfoil, especially at AoA≥3º. The slat can increase the C_l airfoil by flowing fluid from the slat and the main airfoil gap. The narrow slit can accelerate the fluid flow velocity as described in the continuity equation, where the cross-sectional width is inversely proportional to the fluid flow velocity. The slat can also increase fluid velocity by directing the fluid flowing over the top surface of the slat. By Bernoulli's principle, if the velocity of an incompressible fluid increases, the resulting pressure will be lower. This pressure drop will make the difference in fluid pressure between the lower side and upper side bigger so that the airfoil gets a more significant C_l. The effect of using single slat and double slat is not significant when the AoA of the airfoil is at AoA less than 10º. When the AoA of the airfoil exceeds 10º, the difference between the use of a single slat and a double slat becomes more apparent. In order to know in more detail about the difference in extra C_l produced by single slat and double slat, you can review table 1. Table 1 shows the percentage increase in C_l after slat mounted on NACA 4415. The data used as reference data in calculating the increase in C_l is computational data from airfoils without slats. From table 1, it can be seen that at 0°≤AoA≤3°, the use of single slat and double slat was not satisfactory, where the increase in C_l was less than 5%. At AoA>3°, both single slat and double slat increased C_l more than 10%. At 3°≤AoA≤10°, the difference in the ability to increase C_l between the single slat and double slat is always less than 5%. Thus, it can be concluded that at 3°≤AoA≤10°, double slats cannot significantly impact the use of single slats. On the other hand, at 11°≤AoA≤20°, the difference in the percentage increase in C_l between the single slat and double slat is always more than 5%, even at AoA=13° and 14° the percentage increase in C_l from double slat is two times the percentage increase in C_l in the single slat. Overall if done on average to the percentage increase in C_l, a single slat can increase C_l by 20.9129%, while a double slat increase C_l by 25.6878%.

The function of the slat as a flow control device also plays an essential role in improving the performance of the airfoil. Like other fluid flow control devices, slat work by controlling fluid flow separation. Fluid flow separation can be in the form of a complete separation of the boundary layer from the surface of the airfoil, or it can also be in the form of fluid flow bubbles. Fluid flow separation can significantly reduce airfoil C_l or known as stall condition. The ability of the slat to delay the stall can be seen in Figure 5. Single slat and double slat can be delayed until AoA=20º, whereas before using the slat, the airfoil has stalled at AoA=16º.

Slat can increase the dimensions of the airfoil. Larger dimensions mean that it can increase the drag force obtained by the airfoil. However, C_d increase becomes an advantage in some instances, such as an airplane landing. An increase in C_d can be advantageous because it can slow the aircraft's velocity so that the aircraft requires a shorter trajectory to make a landing. The effect of single slat and double can be seen in Figure 5(b). The increase in C_d begins at AoA>12º, where the greater the AoA, the greater the increase in C_d. When AoA 12º, the use of single slat and double slat did not significantly impact the increase in C_d. Meanwhile, the difference in C_d produced by airfoils with single slat and double slat began to be seen at AoA≥17º. The percentage increase in C_d when the airfoil uses single slat and double slat can also be seen in table 1. The average percentage increase in C_d in single slat double slat (26.1109%) is about twice as high as in single slat (54.6152%). Figure 6 is made to determine the optimum AoA of the airfoil. The maximum AoA is obtained at AoA, which results in the peak of the curve. In the ratio curve between C_l to C_d, the optimum AoA is obtained at the peak AoA of the curve. In the airfoil without slats, the optimum AoA of the airfoil is obtained when AoA=6º. Using a single slat can delay the optimum AoA to AoA=7º, while using a double slat makes the optimum AoA to 8º. The peak of the curve on the single slat airfoil is the highest among the others. The reason is that the C_l produced is much more significant than C_d. The use of a double slat contrasts with a single slat, where the peak of the airfoil curve reaches the smallest value compared to the airfoil curve with a single slat and without a slat. So, it can be concluded that double slat makes C_d more dominant. Thus, based on this analysis, using a single slat is more recommended than using a double slat.

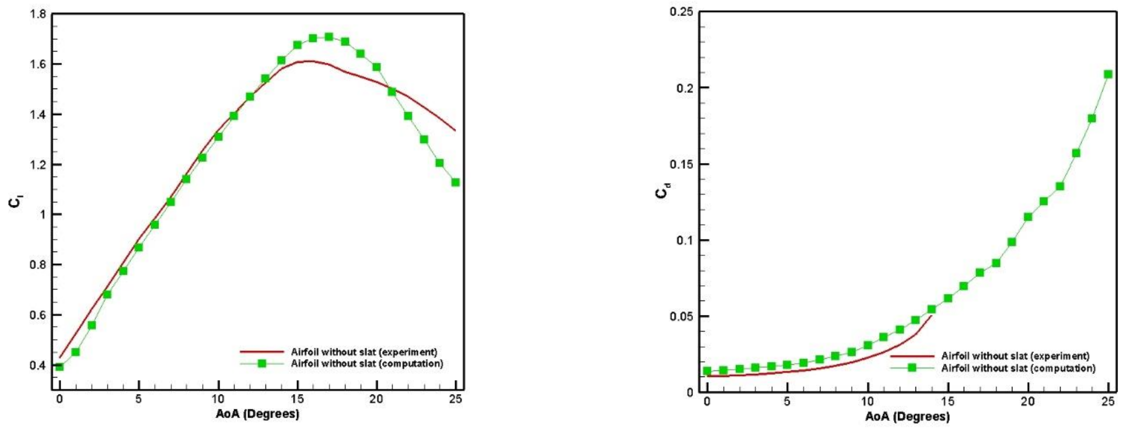

(a) Validation of C_l (b) Validation of C_d

Figure. 4. Aerodynamics validation

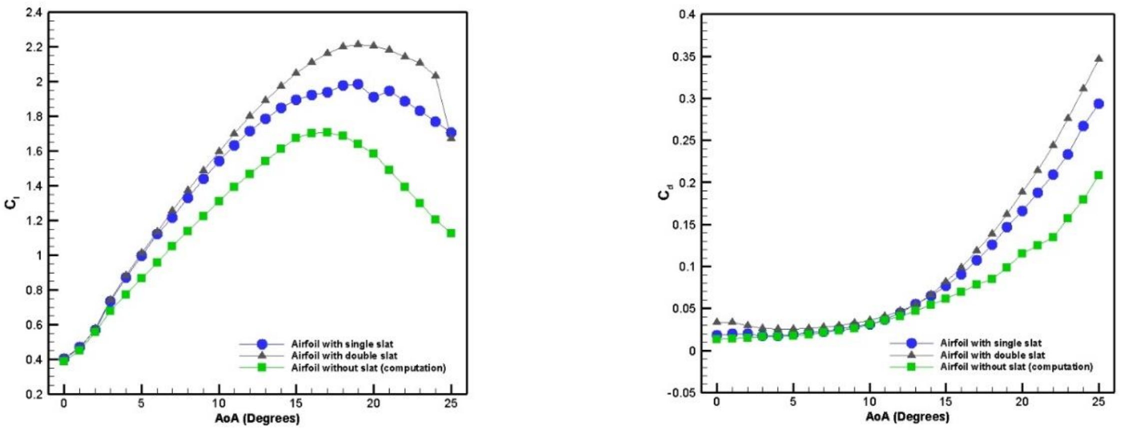

(a) C_l (b) C_d

Figure. 5. Aerodynamic forces of NACA 4415 with single slat, double slat and without slat

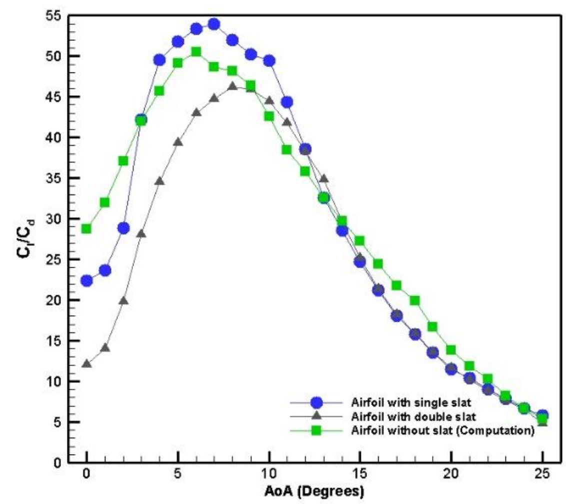

Figure. 6. The ratio between C_l to C_d

TABLE 1.
PERCENTAGE INCREASE IN C_l AND C_d OF SINGLE SLAT AND DOUBLE SLAT

AoA	C_l		C_d	
	Single slat	Double slat	Single slat	Double slat
0	10.3733%	2.0059%	32.2273%	146.9873%
1	7.2728%	6.4802%	40.9794%	135.4383%
2	5.6258%	2.4557%	31.8356%	94.1999%
3	9.0968%	7.6150%	7.0657%	63.3477%
4	14.1530%	12.7482%	3.9653%	51.1494%
5	16.7527%	15.0685%	9.0397%	45.7325%
6	18.3421%	17.0718%	10.7733%	39.0710%
7	19.5297%	15.9756%	4.6366%	30.0412%
8	20.4121%	16.5930%	7.9904%	25.6120%
9	21.1695%	17.5020%	8.5568%	22.6273%
10	21.8657%	17.6655%	1.3368%	16.9369%
11	22.2039%	17.2853%	1.7529%	12.6892%
12	22.5883%	16.7978%	8.5012%	14.5544%
13	15.8678%	22.7584%	16.1254%	15.1045%
14	14.4498%	22.4313%	19.3628%	23.0562%
15	13.1013%	22.3670%	24.8076%	32.5122%
16	12.9828%	24.0494%	30.0536%	41.4781%
17	13.5233%	26.7104%	36.6958%	50.9025%
18	17.1773%	30.2293%	47.8937%	63.2948%
19	21.0067%	34.7863%	48.6846%	64.5309%
20	20.3728%	38.9856%	43.9947%	63.7530%
21	30.8121%	46.5392%	49.8426%	71.3039%
22	35.6317%	54.0540%	55.2202%	80.9136%
23	41.2711%	62.5434%	48.5280%	75.5776%
24	46.7685%	68.6438%	48.4707%	73.1310%
25	51.3840%	48.5192%	40.5432%	66.0502%
$\overline{X}$	20.9129%	25.6878%	26.1109%	54.6152%

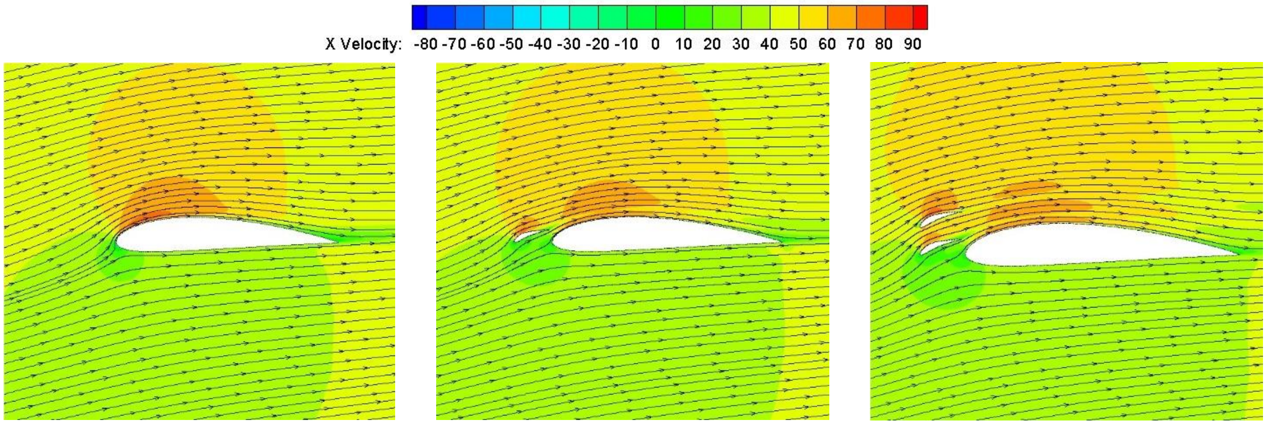

(a) Baseline NACA 4415 at AoA=10º (b) NACA 4415 with single slat at AoA=10º (c) NACA 4415 with double slat at AoA=10º

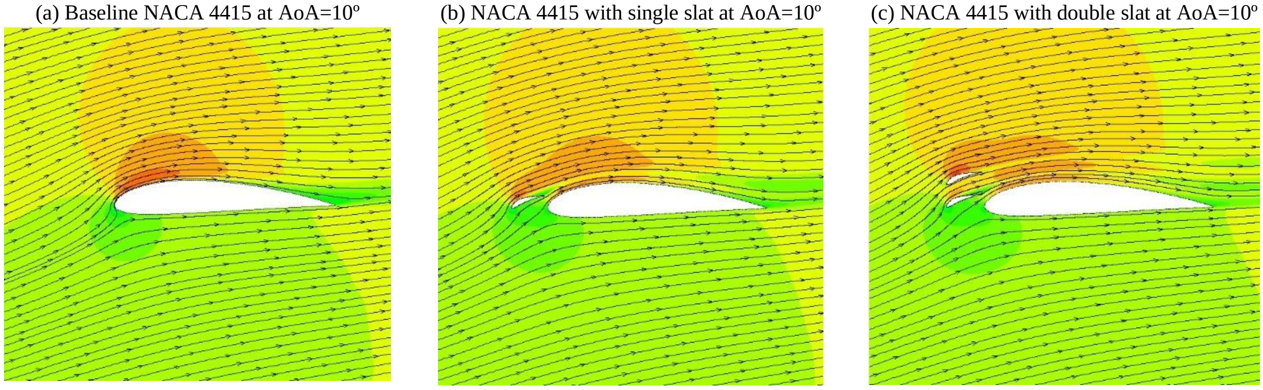

(d) Baseline NACA 4415 at AoA=13º (e) NACA 4415 with single slat at AoA=13º (f) NACA 4415 with double slat at AoA=13º

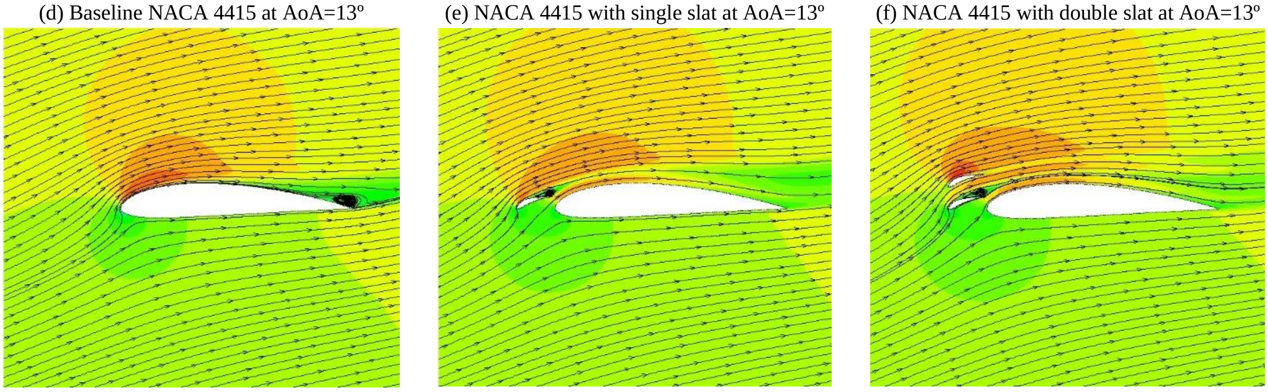

(g) Baseline NACA 4415 at AoA=16º (h) NACA 4415 with single slat at AoA=16º (i) NACA 4415 with double slat at AoA=16º

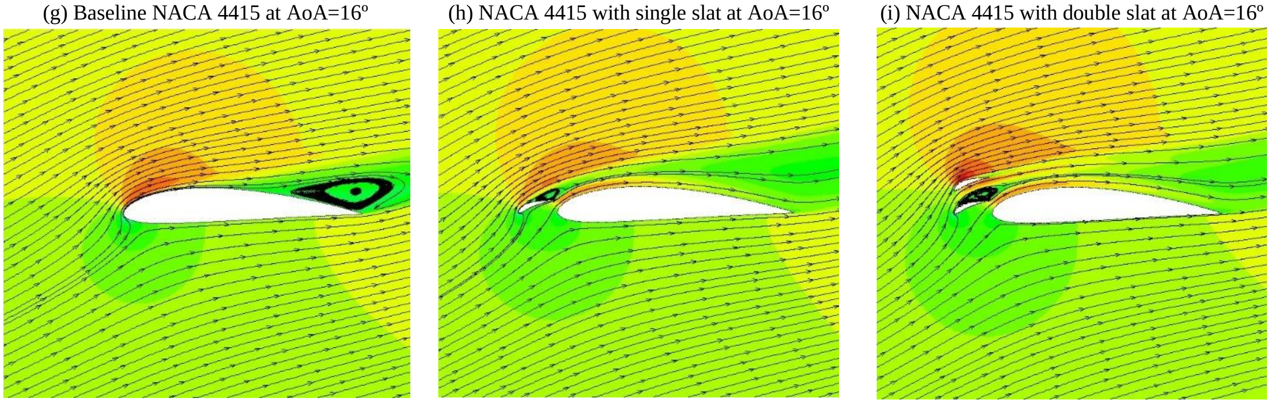

(j) Baseline NACA 4415 at AoA=16º (k) NACA 4415 with single slat at AoA=16º (l) NACA 4415 with double slat at AoA=16º

Figure. 7. Velocity contour and streamline on several AoA

Figure 7 is a visualization of velocity contours and velocity streamline of fluid flow around the baseline NACA 4415, NACA 4415 with single slat, and NACA 4415 with double slat. At AoA=10º and AoA=13º, the fluid flow can follow the airfoil's shape very well so that the airfoil has not experienced a stall condition. Slat can accelerate fluid flow so that the high-speed area becomes wider. When AoA=16º, fluid flow separation begins to form near the trailing edge of NACA 4415. Fluid flow separation forms a circulating fluid flow area in a streamlined form. This fluid flow separation can cause a stall of NACA 4415. Single slat and double slat can eliminate fluid flow separation near the trailing edge of the main airfoil. The picture below shows that the slat eliminates fluid flow separation by directing the fluid to flow near the upper side of NACA 4415. There is no significant difference between the single slat and double slat use at AoA=16º. Fluid flow recirculation is formed near the tail of the slat. The use of a double slat cannot eliminate this fluid flow recirculation. However, the recirculation of fluid flow near the slat does not significantly impact the performance of NACA 4415. When the AoA of the airfoil is increased to 20º, the recirculation of fluid flow at the baseline airfoil becomes larger and worsens its aerodynamic performance. Fluid flow recirculation in the slat also expands almost to cover the entire upper side of the slat. Double slats cannot overcome fluid flow recirculation in the first upper side slat and can even enlarge the fluid flow recirculation area.

IV. CONCLUSION

The research in this paper is a study that focuses on the aerodynamics of the NACA 4415 airfoil. The use of slats can delay the stall. However, stalls in single slat and double slat occurred at the same AoA. In addition, the use of single slat and double slat at AoA before stall can increase C_l NACA 4415 but not significantly. The percentage increase in C_l for airfoils with double slats was 25.6878%, while the percentage increase in C_l for airfoils with single slats was 20.9129%. Using a single slat at AoA≤13° did not significantly affect Cd. The increase in C_d produced by airfoils with a double slat at 0°≤AoA≤3° is more pronounced than at 4°≤AoA≤13° intervals. In general, slat produces a negative effect in the form of an increase in the value of Cd. The average increase in C_d for airfoils with double slats is twice the increase in the single slat. Through C_l/C_d analysis, a single slat can improve the aerodynamic performance of an airfoil better than a double slat. Based on fluid flow visualization, fluid flow separation is formed on the upper side of the airfoil without a slat. The fluid flow separation can be handled well by single slat and double slat, but the effects of single slat and double slat are not too different. Overall, it can be concluded that double slats are not very effective, so it would be better to use a single slat.

REFERENCES

[1] Sarjito, N. Aklis, and T. Hartanto, "An optimization of flap and slat angle airfoil NACA 2410 using CFD," *AIP Conf. Proc.*, vol. 1831, no. April, 2017, doi: 10.1063/1.4981179.

[2] J. Julian, Harinaldi, Budiarso, C. C. Wang, and M. J. Chern, "Effect of plasma actuator in boundary layer on flat plate model with turbulent promoter," *Proc. Inst. Mech. Eng. Part G J. Aerosp. Eng.*, vol. 232, no. 16, pp. 3001–3010, 2018, doi: 10.1177/0954410017727301.

[3] S. Sudhakar and N. Karthikeyan, "Flow Separation Control on a NACA-4415 Airfoil at Low Reynolds Number," *Lect. Notes Mech. Eng.*, no. April, pp. 323–334, 2021, doi: 10.1007/978-981-15-5183-3_35.

[4] T. Yavuz, E. Koç, B. Kilkiş, T. Erol, C. Balas, and T. Aydemir, "Performance analysis of the airfoil-slat arrangements for hydro and wind turbine applications," *Renew. Energy*, vol. 74, pp. 414–421, 2015, doi: 10.1016/j.renene.2014.08.049.

[5] M. Schramm, B. Stoevesandt, and J. Peinke, "Simulation and Optimization of an Airfoil with Leading Edge Slat," *J. Phys. Conf. Ser.*, vol. 753, no. 2, 2016, doi: 10.1088/1742-6596/753/2/022052.

[6] Harinaldi, A. S. Wibowo, J. Julian, and Budiarso, "The comparison of an analytical, experimental, and simulation approach for the average induced velocity of a dielectric barrier discharge (DBD)," *AIP Conf. Proc.*, vol. 2062, no. 1, p. 20027, 2019, doi: 10.1063/1.5086574.

[7] J. Julian, R. F. Karim, Budiarso, and Harinaldi, "Review: Flow control on a squareback model," *Int. Rev. Aerosp. Eng.*, vol. 10, no. 4, pp. 230–239, 2017, doi: 10.15866/irease.v10i4.12636.

[8] A. Choudhry, M. Arjomandi, and R. Kelso, "A study of long separation bubble on thick airfoils and its consequent effects," *Int. J. Heat Fluid Flow*, vol. 52, pp. 84–96, 2015, doi: 10.1016/j.ijheatfluidflow.2014.12.001.

[9] F. C. Megawanto, Harinaldi, Budiarso, and J. Julian, "Numerical analysis of plasma actuator for drag reduction and lift enhancement on NACA 4415 airfoil," *AIP Conf. Proc.*, vol. 2001, 2018, doi: 10.1063/1.5049992.

[10] Budiarso, Harinaldi, Karim, Riza Farrash, and Julian, James, "Drag reduction due to recirculating bubble control using plasma actuator on a squareback model," *MATEC Web Conf.*, vol. 154, p. 1108, 2018, doi: 10.1051/matecconf/201815401108.

[11] Budiarso, Harinaldi, E. . Kosasih, R. . Karim, and J. Julian, "Drag reduction by combination of flow control using inlet disturbance body and plasma actuator on cylinder model," *J. Mech. Eng. Sci.*, vol. 13, no. 1, pp. 4503–4511, 2019.

[12] J. Julian, Harinaldi, Budiarso, R. Difitro, and P. Stefan, "The effect of plasma actuator placement on drag coefficient reduction of Ahmed body as an aerodynamic model," *Int. J. Technol.*, vol. 7, no. 2, pp. 306–313, 2016, doi: doi.org/10.14716/ijtech.v7i2.2994.

[13] Harinaldi, Budiarso, J. Julian, and M. N. Rabbani, "The effect of plasma actuator on the depreciation of the aerodynamic drag on box model," *AIP Conf. Proc.*, vol. 1737, 2016, doi: 10.1063/1.4949292.

[14] Harinaldi, M. D. Kesuma, R. Irwansyah, J. Julian, and A. Satyadharma, "Flow control with multi-DBD plasma actuator on a delta wing," *Evergreen*, vol. 7, no. 4, pp. 602–608, 2020, doi: 10.5109/4150513.

[15] H. Harinaldi, B. Budiarso, F. C. Megawanto, R. F. Karim, N. T. Bunga, and J. Julian, "Flow Separation Delay on NACA 4415 Airfoil Using Plasma Actuator Effect," *Int. Rev. Aerosp. Eng.*, vol. 12, no. 4, pp. 180–186, 2019, doi: doi.org/10.15866/irease.v12i4.16219.

[16] S. M. A. Aftab, A. S. M. Rafie, N. A. Razak, and K. A. Ahmad, "Turbulence model selection for low reynolds number flows," *PLoS One*, vol. 11, no. 4, pp. 1–15, 2016, doi: 10.1371/journal.pone.0153755.

[17] A. J. Lew, G. C. Buscaglia, and P. M. Carrica, "A Note on the Numerical Treatment of the k-epsilon Turbulence Model," *Int. J. Comut. Fluid Dyn.*, vol. 14, no. 3, pp. 201–209, 2001, doi: 10.1080/10618560108940724.

[18] E. N. Jacobs and A. Sherman, "Airfoil section characteristics as affected by variations of the Reynolds number," *Tech. rep., Washington. D.C Natl. Advis. Comm. Aeronaut.*, no. 586, pp. 227–259, 1939.